International Journal of Nanomedicine

Dovepress
open access to scientific and medical research

Open Access Full Text Article

ORIGINAL RESEARCH

Construction of catechol-grafted chitosan alginate/barium sulfate microcapsules for computed tomography real-time imaging and gastroretentive drug delivery

This article was published in the following Dove Press journal:
International Journal of Nanomedicine

Fengyi Du[1,2,*]
Yunchao Wu[2,*]
Fengting Du[3,*]
Lirong Zhang[3]
Weiwei Feng[4]
Lulu Zhao[2]
Rong Cai[3]
Lixia Xu[2]
Gaorui Bian[5]
Jiangang Li[5]
Shengqiang Zou[1]
Aihua Gong[2]
Miaomiao Zhang[2]

[1]Department of Hepatosis, The Affiliated Third Hospital of Zhenjiang, Jiangsu University, Zhenjiang 212013, People's Republic of China; [2]School of Medicine, Jiangsu University, Zhenjiang 212013, People's Republic of China; [3]Department of Physiotherapy, Huangnihe Town Hospital, Huangnihe 133704, People's Republic of China; [4]School of Environmental and Safety Engineering, Jiangsu University, Zhenjiang 212013, People's Republic of China; [5]Tianyi Health Sciences Institute (Zhenjiang) Co. Ltd, Zhenjiang 212013, People's Republic of China

*These authors contributed equally to this work

Correspondence: Miaomiao Zhang
School of Medicine, Jiangsu University, Zhenjiang 212013, People's Republic of China
Email 1000003928@ujs.edu.cn

Background: The gastroretentive drug delivery system is an effective administration route, which can improve the bioavailability of the drug and the therapeutic effect by prolonging the release time of the drug and controlling the release rate in the stomach.

Methods: Inspired by the excellent adhesion properties of mussel protein, we prepared novel catechol-grafted chitosan alginate/barium sulfate microcapsules (Cat-CA/BS MCs) with mucoadhesive properties and computed tomography (CT) imaging function for gastric drug delivery. First, barium sulfate nanoclusters used as CT contrast agent were synthesized in situ in the Cat-CA/BS MCs through a one-step electronic spinning method. Next, catechol-grafted chitosan as the mucoadhesive moiety was coated on the surface of Cat-CA/BS MCs by polyelectrolyte molecule self-assembly.

Results: The prepared Cat-CA/BS MCs could effectively retained in the stomach for 48 hours and successively released ranitidine hydrochloride, which could be used for the treatment of gastric ulcer. Cat-CA/BS MCs exhibited superior CT contrast imaging properties for real-time tracking in vivo after oral administration.

Conclusion: These findings demonstrate that Cat-CA/BS MCs serving as multifunctional oral drug carriers possess huge potential in gastroretentive drug delivery and non-invasive visualization.

Keywords: catechol, mucoadhesive, microcapsules, CT imaging, gastroretentive drug delivery

Introduction

Oral administration is one of the most common routes of administration for digestive tract diseases. However, owing to various factors such as gastric peristalsis and gastric emptying, most drugs are rapidly discharged into the duodenum from the stomach. Traditional medicine is difficult to maintain in locally high concentrations, so the bioavailability of some drugs is greatly reduced. Moreover, the strong first-pass effect, the poor specificity, and the large fluctuation in blood concentration, indicate that many patients cannot be fully treated.[1] Conventional oral delivery systems have significant limitations on drugs with low solubility, absorption sites primarily in the stomach and the proximal part of the small intestine, and the need for continuous administration to the colon.[2] Although progress on gastroretentive systems, including mucoadhesive, high-density, expandable, and floating systems, has been made, they still suffer from low efficiency, poor biocompatibility, and

submit your manuscript | www.dovepress.com
DovePress
http://doi.org/10.2147/IJN.S204237

complex fabrication methods.[3–6] Therefore, prolonging the residency time of the drug in the stomach and improving the bioavailability of the drug are key factors in oral formulation technology.

Microcapsules (MCs), which originated in the 1950s, are small containers with a core–shell structure,[7,8] comprising the internal core material and external wall material. Preparation of MCs mainly includes spray drying, in situ polymerization, emulsion cross-linking, and organic solvent phase separation.[9] MC preparation technology has developed rapidly and has matured in recent decades. MCs have been widely used in many fields, such as biomedicine, and drawn wide attention around the world because of their good biodegradability and biocompatibility. The network structure of the MCs' wall improves the stability and allows for sustained-release drugs, reduced drug damage and stomach stimulation, and other features.[10] Our previous work reported a novel MC with intestinal targeting and computed tomography (CT) tracking features for oral probiotic delivery.[11] However, currently, conventional oral drugs have no target selectivity and have a short drug maintenance time, which is not conducive to the treatment of local damage and has a negative impact on treatment and prognostic evaluation.

Mussels are one of the most common organisms in the ocean, and can firmly adhere to the surface of various materials in a humid environment. Their secreted silk fibroin has features of extensive adhesiveness, high strength, high tenacity, and water resistance.[12] Numerous studies have confirmed that the main functional elements are 3,4-dihydroxyhydrocinnamic acid (also known as Dopa) and positive amino acids (such as lysine). Based on these findings, catechol derived from a side chain of the Dopa molecule has been considered an ideal candidate for construction of mucoadhesive materials. The advantages of using catechol are that catechol derivatives are commercially available for bioconjugation to amine and carboxylic acid groups, and that catechol can form irreversible covalent bonds with thiols and amine via oquinone by catechol oxidation.[13–15] In addition, the unique molecular structure of catechol, being an interfacing intermediary between proteins, mediating the covalent cross-links between proteins, and other characteristics of the substrate, make it a promising adhesive material.[16]

Inspired by its excellent adhesive performance, the biodegradable and biocompatible biomimetic catechol-based material has been extensively applied in wearable devices, conductive hydrogels, biosensors, and buccal drug delivery methods.[17–19] Related studies have explored the role of catechol in bioadhesion, as a bioadhesive material with significant advantages and potential.[20] However, no further studies have been conducted to apply the mucoadhesive catechol for gastric retention in drug delivery. Therefore, we combined MCs with mucoadhesive molecules and non-invasive imaging agents to fabricate a novel kind of multifunctional MC.[21] The as-synthesized MCs exhibited a strong capability for adhering to the surface of gastric mucosa and enabled sustained release of drugs to treat gastric disease. To monitor this process in real time, barium sulfate, as a non-invasive imaging contrast agent, was produced in situ in the MCs for the first time.

Materials and methods

Materials

Chitosan (CS; deacetylation ≥95%, viscosity 100–200 mPa.s), N-(3-dimethylaminopropyl)-N'-ethylcarbodiimide hydrochloride (EDC; ≥98.5%), sodium alginate, ranitidine hydrochloride (RH), and ammonium acetate (≥99.0%) were purchased from Aladdin Industrial (Shanghai, China). 3,4-Dihydroxyhydrocinnamic acid (≥98%) was purchased from Sigma-Aldrich (St Louis, MO, USA). Solar Fluor 750 SE was purchased from Beijing Solarblo Science & Technology Co. (Beijing, China). Mucin type II was purchased from Macklin Biochemical Technology Co. (Shanghai, China). Barium chloride dihydrate, sodium sulfate anhydrous, trisodium citrate dihydrate, sodium chloride, acetic acid, methanol, and ethanol were purchased from Sinopharm Chemical Reagent Co. (Shanghai, China). All other chemicals and reagents were of analytical grade.

Synthesis of catechol–chitosan (Cat-CS)

Cat-CS was synthesized in a similar way to previous reports.[13,22] In brief, 3.25 mmol chitosan was dissolved in distilled and deionized water (DDW) containing 0.4 mL acetic acid; after sufficient dissolution 40.5 mL DDW was slowly added and the solution pH was adjusted to about 4.5 with 1 N NaOH. Then, 3.25 mmol of 3,4-dihydroxyhydrocinnamic acid dissolved in 5 mL DDW was added. 6.49 mmol of EDC was dissolved in a mixed solution of 50 mL of DDW and ethanol (v:v=1:1) and added dropwise to the previously obtained mixed solution at a pH of 5.0, then vigorously stirred at room temperature for 4 hours. The mixed

solution after the reaction was transferred to a dialysis membrane tube (molecular weight cut-off: 2,000; Union Carbide, Bound Brook, NJ, USA) in DDW of pH 5.0 for 2 days, followed by 4 hours in PBS and 1 day in DDW. Finally, the sample was freeze-dried and collected. The above procedure was repeated using 3.25 mmol chitosan, 3.25 mmol 3,4-dihydroxyhydrocinnamic acid, and 3.25 mmol EDC; and 3.25 mmol chitosan, 3.25 mmol 3,4-dihydroxyhydrocinnamic acid, and 4.20 mmol EDC.[13] The degree of conjugation of catechol at the chitosan side chain was determined by an ultraviolet–visible (UV-Vis) spectrophotometer (Cary 8454, USA) and the absorption intensity was measured at a wavelength of 280 nm. The resulting products were named Cat6-CS, Cat13-CS, and Cat27-CS, according to the degree of conjugation.

Characterization of Cat-CS and MCs

A UV-Vis spectrophotometer (Cary 8454, USA) was used to analyze the composition of the Cat-CS. A Fourier transform infrared (FT-IR) spectrometer (Nicolet Nexus 470; GMI, Ramsey, MN, USA) was used to analyze the types of functional groups contained in the Cat-CS and the chemical environment in which it is located. Nuclear magnetic resonance (^{1}H-NMR) spectroscopy (AVANCE II, 400 MHz, Bruker, Switzerland) was used to analyze the composition and structure of the Cat-CS.

Fabrication of catechol-grafted chitosan alginate/barium sulfate microcapsules (Cat-CA/BS MCs)

First, alginate microspheres with barium sulfate (A/BS MSs) were prepared by electrostatic spraying (20 V, 55 mL/hour) using mixed aqueous solution including 1% (w/v) sodium alginate and 0.5% (w/v) anhydrous sodium sulfate as the injection solution, and 4% (w/v) barium chloride dihydrate as the receiving solution.[23] After washing three times using DDW, the MSs were immersed in 1% (w/v) chitosan aqueous solution for 1 hour, then 0.2% (w/v) sodium alginate aqueous solution for 10 minutes. Next, the obtained MSs continued to be immersed into 1% (w/v) CS, Cat6-CS, Cat13-CS, and Cat27-CS aqueous solution for 1 hour. Finally, CA/BS MCs and Cat-CA/BS MCs were obtained after 1% (w/v) trisodium citrate dehydrate liquidation for 5 minutes. The as-prepared MCs were freeze-dried and stored at 4°C.

Optimization of barium sulfate in the MCs

Using an electrostatic spraying method, 0.1%, 0.3%, 0.5%, and 1.0% anhydrous sodium sulfate mixed with 1% sodium alginate was sprayed into the receiving solution containing 4% barium chloride solution to prepare four kinds of MCs. The morphological structure of each group of MCs was assessed, and then the transverse section of each group of MCs was observed by scanning electron microscopy (SEM) (Zeiss Merlin Compact, Oberkochen, Germany).

Characterization of barium sulfate crystal in the MCs

A field emission SEM (Zeiss Merlin Compact) was used to observe the micromorphology of barium sulfate nanocrystals in the MCs. An X-ray diffraction (XRD) instrument was used to measure the crystal structure of barium sulfate in situ synthesized in MCs, with 2θ ranging from 5.0° to 90.0° in steps of 0.02° under Cu Kα radiation. The MCs with gradient barium sulfate crystals were scanned by CT to detect different CT imaging effects.

Characterization of binding behavior between catechol-grafted chitosan (Cat-CS) and mucin using surface plasmon resonance (SPR)

An SPR test (Biacore 3000; Bioscience, USA) was used to study the adhesion properties between CS/Cat27-CS and mucin. CS and Cat27-CS were each dissolved in PBS (pH 2) at a concentration of 1 mg/mL. Mucin was dissolved in PBS (pH 2) with stirring and ultrasound for 20 minutes, at a concentration of 1 mg/mL. The flow rate of mucin was 10 μL/minute, PBS (pH 7.4) washing was carried out after 15 minutes of mucin adsorption, then CS and Cat27-CS were injected at a flow rate of 30 μL/minute.[13]

Mucosa adhesion in vitro

Six to eight-week-old female C57BL/6 mice were purchased from Model Animal Genetics Research Center of Jiangsu university, Zhenjiang, People's Republic of China). All efforts were made to minimize animals' sufferingand to reduce the number of animals used. were fasted for 24 hours and then killed by cervical dislocation. Stomach tissues were extracted and the contents were washed away with physiological saline and cut into 1 cm×2 cm pieces, then placed on a glass slide.

A certain number of A/BS MCs, CA/BS MCs, and Cat27-CA/BS MCs were evenly spread on the surface of the gastric mucosa, soaked with physiological saline, and moisturized for 20 minutes in a wet box. After the moisturization, the slides were removed and fixed on a 45°C inclined surface to simulate the MCs adhered to the surface of the gastric mucosa using simulated gastric fluid washing (20 mL/minute) for 5 minutes. After completion of the washing, the number of MCs retained on the surface of the gastric mucosa was counted, and the retention rate was calculated.[24]

Mucosa adhesion in vivo

All animal feeding and experimental protocols were approved by the Animal Management Rules of the Ministry of Health of the People's Republic of China and the Guidelines for the Care and Use of the Jiangsu University Laboratory Animal Center. KM mice (male, 7 weeks old, from Jiangsu University Animal Center) were starved for 24 hours prior to the experiments. Twelve mice were administered, by gavage, with 0.5 mL CA/BS MCs, Cat6-CA/BS MCs, Cat13-CA/BS MCs, and Cat27-CA/BS MCs. CT scanning imaging was performed at 5 minutes, and 1, 3, 6, and 24 hours, observing the positional changes of the MCs in mice at different time-points and performing mucosal adhesion analysis.

Near-infrared (NIR) bioimaging in vivo

NIR dye 1% Solar Fluor 750 (SF750) succinimide (SE) solution was prepared using anhydrous DMSO; the SF750 SE solution was mixed with 1% polyetherimide (PEI) aqueous solution (pH 8.5) (v:v=1:9), and shaken for 1 hour in the dark. Then, the MCs were then immersed in 1% PEI-SF750 SE for 1 hour, 0.2% sodium alginate for 10 minutes, and 1% CS/1% Cat27-CS for 1 hour. Mice were orally administered equal amounts of NIR CA/BS MCs and Cat27-CA/BS MCs.

Drug loading and release

To study the release of RH in the MCs in vitro, we prepared drug-loaded Cat27-CA/BS MSs and Cat27-CA/BS MCs in a simulated gastric fluid. A mixed solution of 1% sodium alginate, 0.5% anhydrous sodium sulfate, and 0.625% RH was injected into a 4% cerium chloride solution by electrostatic spraying to obtain MSs. Then, these MSs underwent surface coating and liquidation to form MCs with RH loading. To study the drug release profiles of RH-Cat27-CA/BS MSs and RH-Cat27-CA/BS MCs, the loading rate of RH first needed to be determined. The supernatant was collected by centrifugal MSs/MCs and the free RH in the supernatant was determined by high-performance liquid chromatography (HPLC).[25] The loading rate of RH was calculated from the following equation:[26]

$$\text{entrapment efficiency} = \frac{\text{total amount of drug} - \text{drug in the supernatant}}{\text{total amount of drug}} \times 100\%$$

Furthermore, the release profiles of RH from MCs were studied in the simulated gastric fluid at 37°C. At set time intervals, samples were removed and the supernatants were collected, then subjected to HPLC. The percentage of the cumulative amount of released RH was determined by a standard calibration curve.[27] The analytical column was an Agilent C18 (250 mm×4.6 mm, 5 μm); The mobile phase comprised methanol/0.5% ammonium acetate solution=(75:25), flow rate was 1 mL/minute, detection wavelength 320 nm, column temperature 25°C, and injection volume 10 μL. Both samples needed to be filtrated using a filter membrane of 0.45 μm.[28]

Treatment of gastric ulcer in mice

Experiments on gastric ulcer treatment in mice were executed according to the protocol approved by the Animal Management Rules of the Ministry of Health of the People's Republic of China and approved by the Institutional Animal Care and Use Committee of Jiangsu University. In this study, the gastric ulcer mouse model was established by acetic acid induction and used to assess MC adhesion and imaging performance. After fasting for 24 hours, the mice (KM mice, male and female, 25±3 g, Jiangsu University Animal Center) were intragastrically given 0.5 mL of water for the first time, and 0.5 mL of water was given 3 hours later, followed by 20% acetic acid solution (0.025 mL/10 g) after 2 hours.[29] The gastric ulcer area caused by this method was large, but the survival rate was 100%.

The mice were divided into six groups (n=6): the negative control group, positive control group (only acetic acid induction), A/BS MCs treatment group, RH treatment group (50 mg/kg, orally),[30] RH-CA/BS MCs treatment group, and RH-Cat27-CA/BS MCs treatment group.[31] During continuous administration for 7 days, the body weight of the mice was recorded every day. Mice were killed by cervical dislocation after 7 days of treatment. The stomach was removed and the gastric mucosal injury index and inhibition rate were evaluated. Scoring was based

on the size of the ulcer or erosion area. 1) Every three point ulcers (if the mucosal defect is <1 mm or the hemorrhagic erosion is small, this is called a point ulcer) recorded 1 point. 2) Strips of bleeding: the product of the maximum long diameter of the ulcer and the maximum width perpendicular to the maximum long diameter is called the ulcer index. The width records 1 point per 1 mm, for lesion widths >4 mm, the number is counted. The sum of the scores of the mucosal lesion length is taken as the ulcer index (if the length of the ulcer is not an integer, the fractional part is rounded off).[32] The weight of each group's stomach tissue was recorded and the percentage of ulcer inhibition was calculated as: Ulcer inhibition rate %= (Control group ulcer index − Administration group ulcer index)/Control group ulcer index ×100%. The gastric lesions and surrounding mucosal tissue were fixed in 4% paraformaldehyde, dehydrated by methanol exposure, embedded in paraffin, sectioned to 10 μm thickness, and then stained with H&E for histological examination.

Statistical analysis

All data are presented as mean ± SD. Statistical comparisons were statistically analyzed by one-way ANOVA. Values of $P<0.05$ were considered statistically significant.

Results

Synthesis and characterization of catechol-grafted chitosan

The catechol-grafted chitosan was synthesized using the N-hydroxysuccinimide (NHS) chemistry method and characterized by UV-Vis spectrophotometry, FT-IR, and NMR. In this study, a series of catechol-grafted chitosan with different grafting degrees from 6 to 27 (noted as Cat6-CS, Cat13-CS, and Cat27-CS) was prepared by adjusting the starting materials ratio. The characteristics of the absorption peak via the UV-Vis spectrum could be used for qualitative or quantitative analysis of catechol grafting degree. Figure 1A shows that Cat6-CS, Cat13-CS, and Cat27-CS all possessed a unique characteristic absorption peak at a wavelength of 280 nm, which was consistent with the UV absorption peak of the benzene ring in the molecular structure of catechol.[22] However, CS lacked the characteristic absorption peak at 280 nm. Next, the catechol-grafted chitosan was identified and analyzed by FT-IR spectroscopy. Figure 1B shows that an intense spectral peak appeared at 3,410 cm^{-1}, which was caused by the stretching and vibration of O–H.[33] Owing to the acetic acid in the solution, a peak at 1,533 cm^{-1} was present in the CS spectrum, which led to amino protonation.[34] The peak of the catechol-grafted chitosan sample at about 1,640 cm^{-1} appeared similar to that of CS, which corresponded to the stretching vibration of the C=C double bond in the carboxyl group. This result verified the existence of catechol in Cat-CS samples.[35] In the spectra of Cat-CS samples, a small peak appeared at 1,740 cm^{-1}, which corresponded to aromatic C=O stretching. The ^{1}H-NMR spectra were used to further confirm that catechol had been grafted on the chitosan backbone.[14,36,37] Figure 1C shows that the three protons clearly visible from 6.5 to 7.0 in the spectra were the proton peaks of benzene in catechol, which was consistent with the pure catechol product. Furthermore, the presence of ^{1}H–^{1}H COZY cross-peaks confirmed that catechol had been successfully modified on the side chain of the chitosan molecule.[22]

Morphological characterization of the Cat-CA/BS MCs

Cat27-CA/BS MCs were successfully fabricated after electrostatic spraying and polyelectrolyte molecule self-assembly, as shown in Scheme 1. To characterize the morphology and size distribution, the as-prepared Cat27-CA/BS MCs were observed by digital camera photography and statistically analyzed.[38] Figure 2 shows that the as-prepared A/BS MSs, CA/BS MCs, and Cat27-CA/BS MCs exhibited a milky white appearance and nearly round shape. After statistical analysis, A/BS MSs, CA/BS MCs, and Cat27-CA/BS MCs had uniform shape and size, with diameters of 610 μm, 580 μm, and 560 μm, respectively. The size of Cat27-CA/BS MCs and CA/BS MCs was smaller than that of A/BS MSs. This phenomenon may be attributed to shrinkage after citric acid liquidation.

Effect of barium sulfate nanocrystals on MC morphology

Barium sulfate nanocrystals are rapidly formed when sulfate ions encounter barium ions in an aqueous solution. To explore the effect of barium sulfate on the MC morphology, different concentrations of sodium sulfate in the injection solution were chosen to fabricate the MCs. In this study, the effect of in situ synthetic barium sulfate nanocrystals on MC morphology was preliminarily observed in natural light, as shown in Figure S1. With the increasing amount of sodium sulfate, the morphology

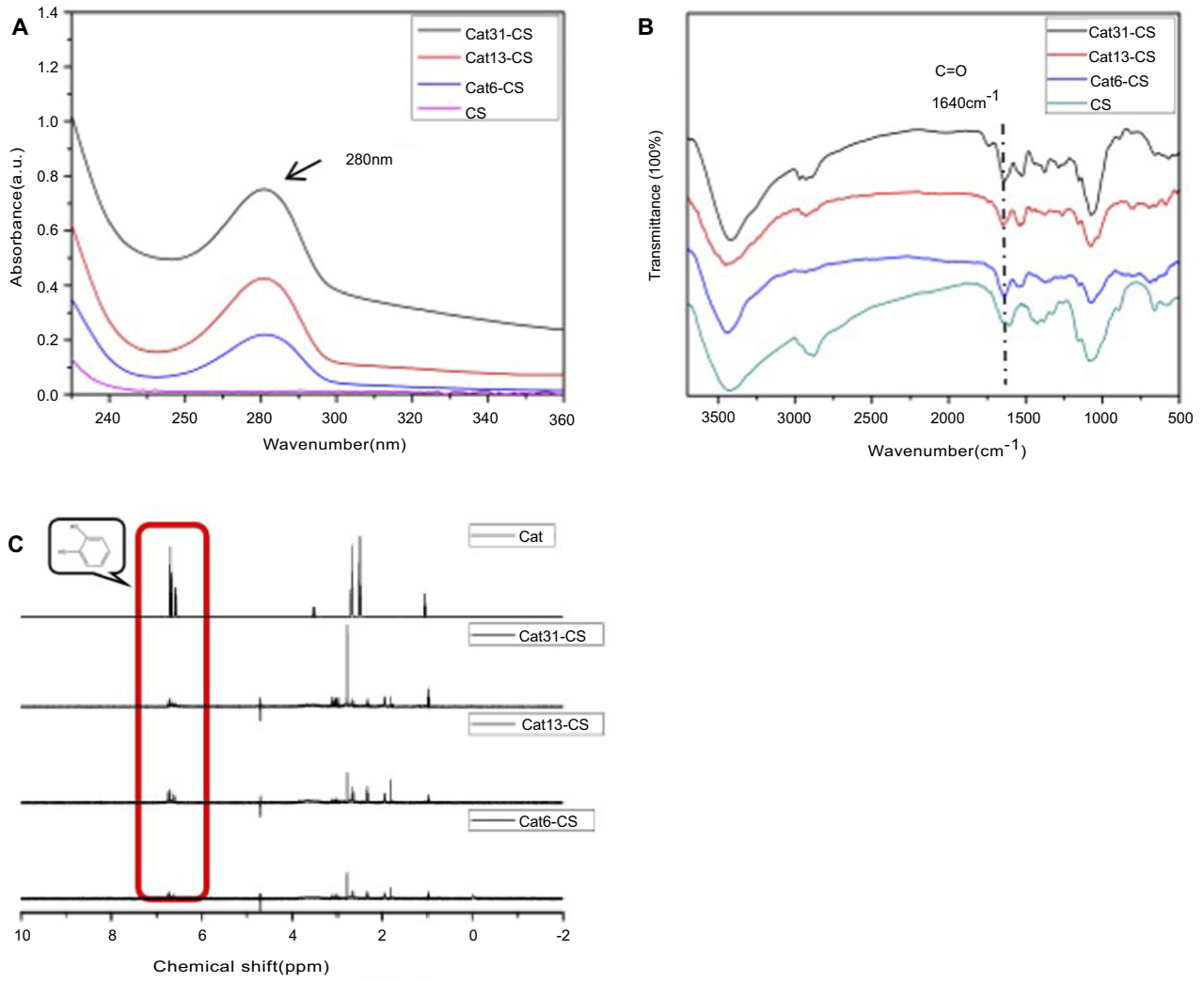

Figure 1 Characterization of Cat-CA/BS MCs. (**A**) UV-Vis spectra of CS, Cat6-CS, Cat13-CS, Cat27-CS. (**B**) FTIR spectra of CS, Cat6-CS, Cat13-CS, Cat27-CS. (**C**) ^{1}H-NMR spectra of Cat6-CS, Cat13-CS, Cat27-CS, catechol.

Abbreviations: Cat-CA/BS MCs, catechol–chitosan/barium sulfate microcapsules; UV-Vis, ultraviolet–visible; CS, chitosan; Cat-CS, catechol–chitosan; FT-IR, Fourier transform–infrared; NMR, nuclear magnetic resonance.

of the prepared Cat27-CA/BS MCs changed significantly. When the concentration of anhydrous sodium sulfate was 0.1, the Cat27-CA/BS MCs with complete external shape were grayish white. When the concentration was 0.3, the Cat27-CA/BS MCs turned light white owing to greater barium sulfate nanocrystal formation. When the amount reached 0.5%, the Cat27-CA/BS MCs turned milky white and suffered a small amount of damage. Most of the Cat27-CA/BS MCs had a spherical form and uniform shape. However, when the anhydrous sodium sulfate concentration reached 1.0%, the Cat27-CA/BS MCs were close to white and about half of their walls were broken. Consequently, their morphologies were incomplete and the breakage rate was as high as approximately 60%. It is concluded that 0.5% sodium sulfate is considered as the optimal condition to generate appropriate barium sulfate nanocrystals for maintaining complete morphology of Cat27-CA/BS MCs.

At the same time, the outer walls of the Cat27-CA/BS MCs generated by different concentrations of sodium sulfate were characterized by SEM. Figure 3 shows that only a trace amount of barium sulfate crystals was formed on the walls of the Cat27-CA/BS MCs in the 0.1% sodium sulfate group. When the concentration of sodium sulfate was 0.3%, clusters of barium sulfate nanocrystals were clearly observed. When the concentration was 0.5%, a large amount of barium sulfate nanocrystals was attached to the wall of the Cat27-CA/BS MCs. When the concentration reached 1.0%, the surface of Cat27-CA/BS MCs was almost covered with barium sulfate nanocrystals and

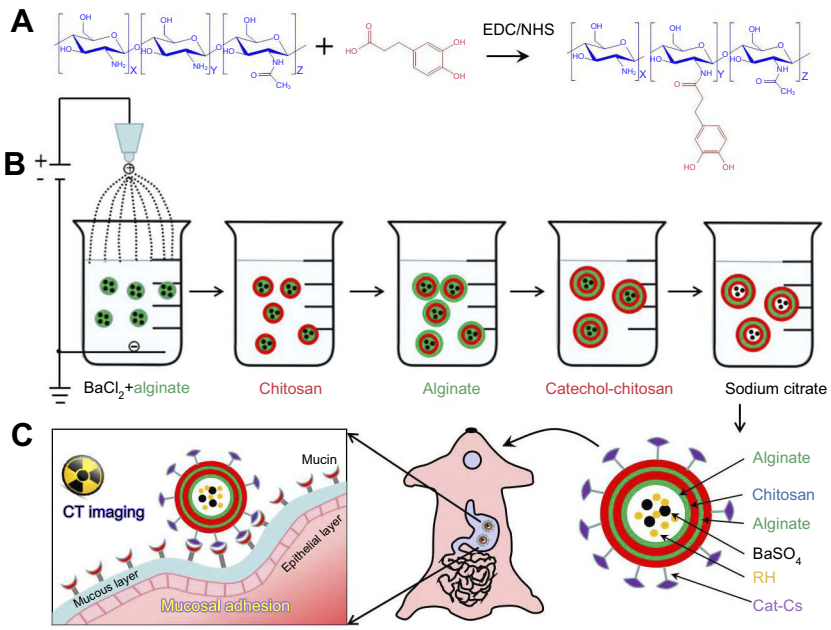

Scheme 1 Schematic illustration of the preparation process of Cat-CA/BS MCs and their applications in gastroretentive drug delivery and CT imaging. (**A**) Preparation of catecholylated chitosan; (**B**) preparation of Cat-CA/BS MCs; (**C**) Cat-CA/BS MCs for CT real-time imaging and mucosal adhesion-mediated gastric drug delivery. **Abbreviations:** Cat-CA/BS MCs, catechol-grafted chitosan alginate/barium sulfate microcapsules; CT, computed tomography; EDC, ethylcarbodiimide hydrochloride; NHS, N-hydroxysuccinimide; RH, ranitidine hydrochloride.

a number of cracks appeared. This concern may be ascribed to the huge surface tension derived from the excessive coverage of barium sulfate nanocrystals. It can be seen that the appropriate amount of barium sulfate nanocrystals is significant for maintaining the integrity of the Cat27-CA/BS MCs group, which could be used to realize the concentration of sodium sulfate in the preparation process.

Physical characterization of barium sulfate crystals and CT imaging in vitro

To better study the physical features, the as-prepared Cat27-CA/BS MCs underwent a freeze-drying process to remove moisture. After lyophilization, Cat27-CA/BS MCs maintained a nearly spherical appearance, indicating that their walls possessed a certain mechanical strength (Figure 4A). As shown in Figure 4B, the surface of the Cat27-CA/BS MCs was generally flat and had a small number of irregular voids, which may be attributed to the formation and disappearance of water crystals during lyophilization. Laser scanning confocal microscopy was used to explore the self-assembly of polyelectrolytes on the surface of MCs. In Figure S2, the binding between the alginate labeled by fluorescein isothiocyanate and the chitosan labeled by rhodamine can be observed, suggesting that the chitosan could self-assemble on the surface of alginate spheres owing to electrostatic interactions. Then, these lyophilized Cat27-CA/BS MCs were sliced open to observe the inner structure using SEM. As can be seen from the pictures, the inner surface of as-prepared Cat27-CA/BS MCs had an abundant scaly structure (Figure 4C), which may be due to citric acid liquidation. Meanwhile, a large number of barium sulfate nanocrystals could be observed after pseudo-color processing on the inner surface of MCs (Figure 4D). These nanocrystals exhibited relatively uniform and nano-scale size distribution, which was of significance for the capability of CT contrast imaging.[39,40]

To reveal whether these barium sulfate nanocrystals synthesized in situ possessed same phase structure as natural barium sulfate, XRD spectrum analysis was conducted using the lyophilized Cat27-CA/BS MCs. By XRD spectrum analysis of barium sulfate crystals, the main diffraction peaks in Figure 4E showed a broad diffraction peak at 42.62°, matching well the structure of the natural orthorhombic barium sulfate crystals. This result demonstrated that barium sulfate crystallites synthesized in situ inside MCs had almost the same phase structure as natural barium sulfate.[11] Furthermore, the X-ray attenuation ability of Cat27-CA/BS MCs in vitro was verified by CT scanning (Figure 4F). As the number of Cat27-CA/BS MCs increased, the CT signal intensity markedly increased. Through quantitative

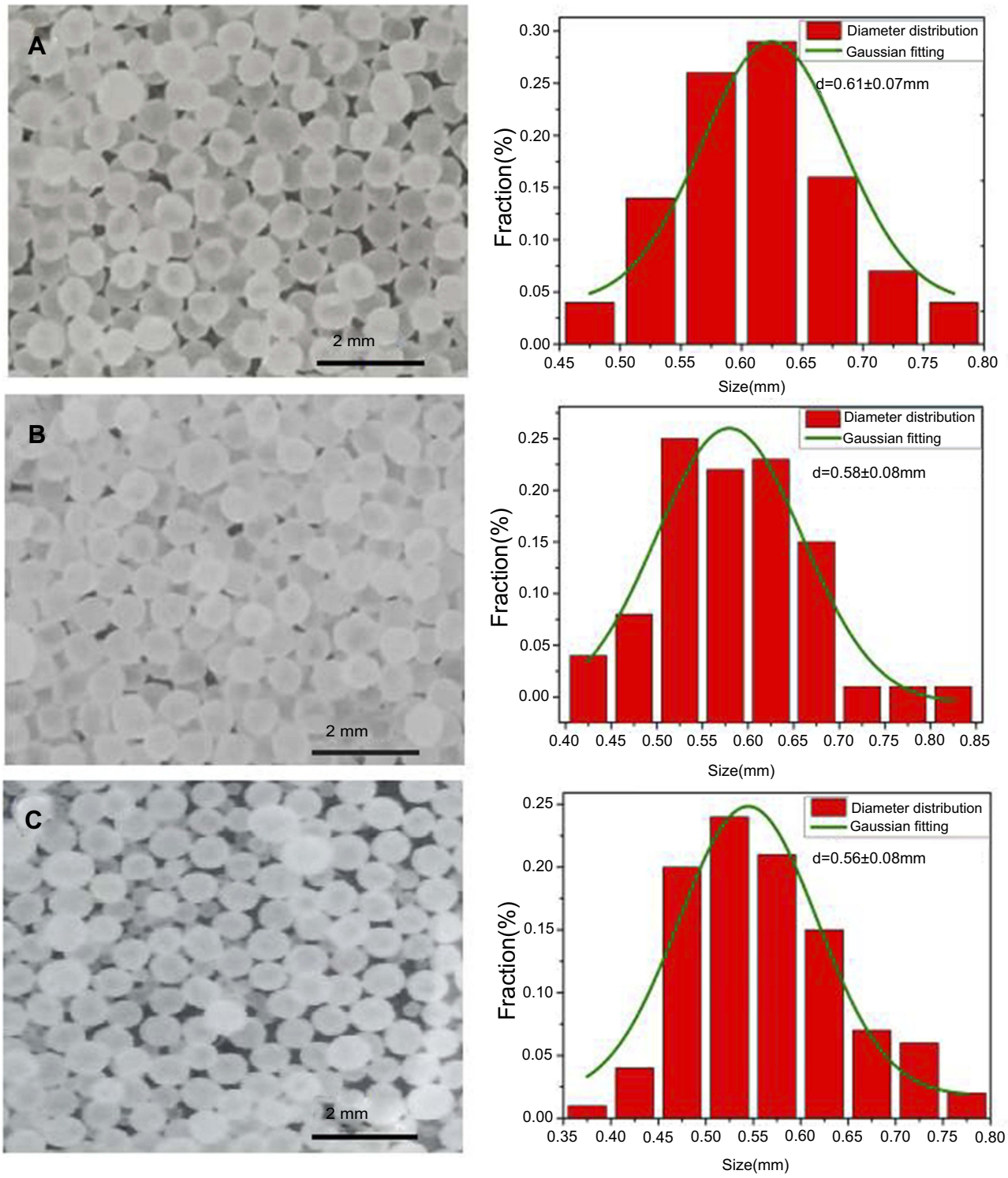

Figure 2 Morphological characterization of microcapsules. Optical images of (**A**) A/BS MSs, (**B**) CA/BS MCs, and (**C**) Cat27-CA/BS MCs in water, and their corresponding size distributions.

Abbreviations: A/BS MSs, alginate/barium sulfate microspheres; CA/BS MCs, chitosan alginate/barium sulfate microcapsules; Cat27-CA/BS MCs, catechol-27–chitosan alginate/barium sulfate microcapsules.

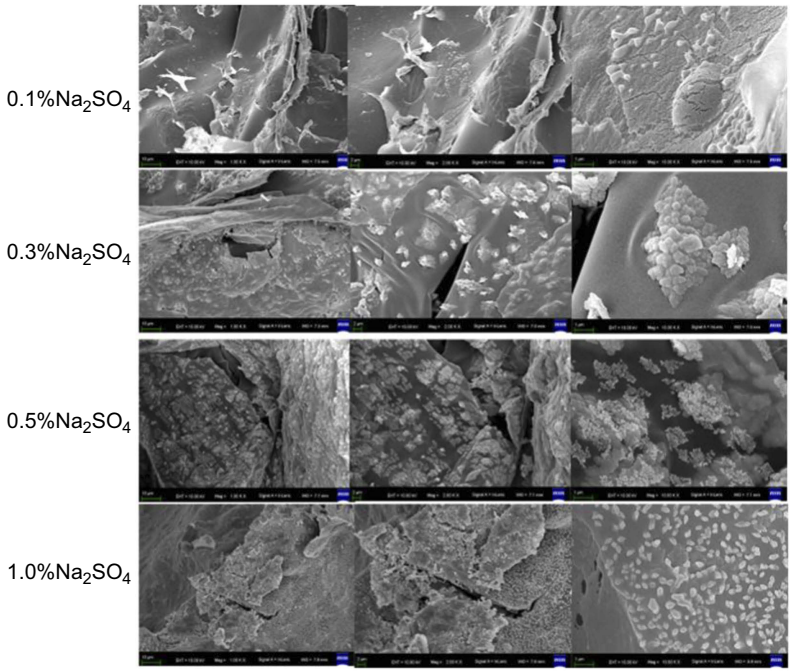

Figure 3 Scanning electron microscopy images of gradient barium sulfate nanocrystals on the wall of the Cat27-CA/BS MCs using a series of concentrations of sodium sulfate as the injection solution.
Abbreviation: Cat27-CA/BS MCs, catechol-27–chitosan alginate/barium sulfate microcapsules.

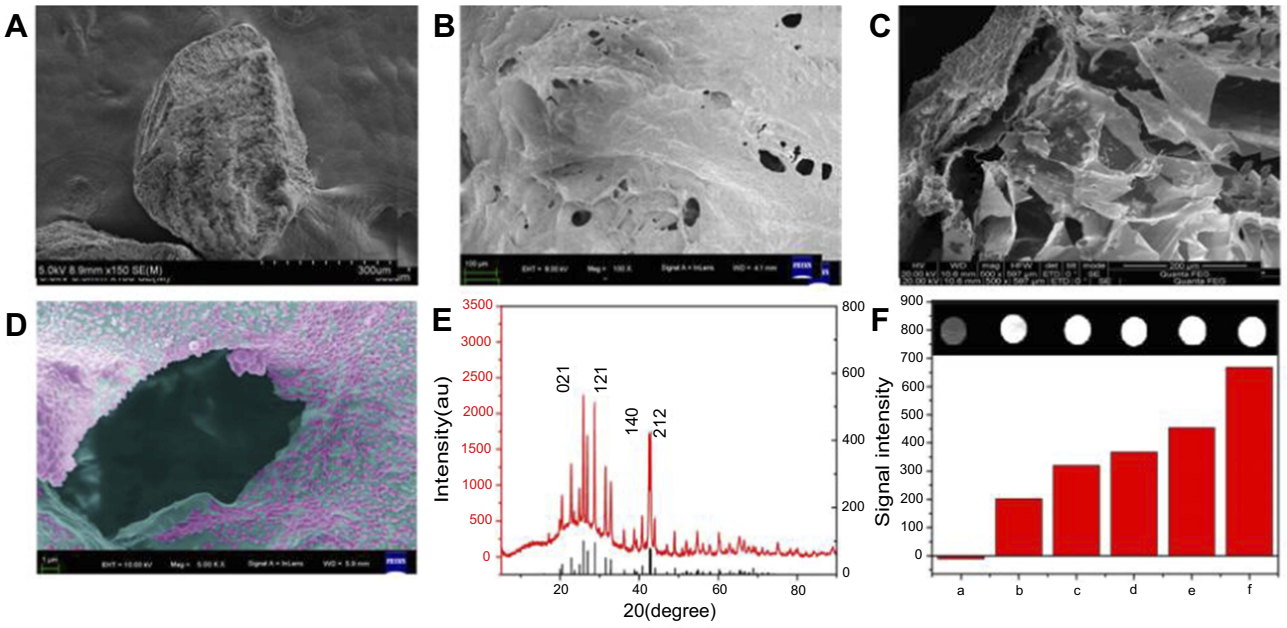

Figure 4 Morphological characterization of Cat27-CA/BS MCs. (**A** and **B**) SEM images of outside surface of MCs. (**C**) SEM image of wall structure of MCs. (**D**) SEM image of barium sulfate crystal nanoclusters on the inside surface of Cat27-CA/BS MCs (pseudo-color). (**E**) X-ray diffraction pattern of Cat27-CA/BS MCs. (**F**) In vitro CT imaging of Cat27-CA/BS MCs with varying content.
Abbreviations: Cat27-CA/BS MCs, catechol-27–chitosan alginate/barium sulfate microcapsules; SEM, scanning electron microscopy; CT, computed tomography.

analysis using ImageJ software, the CT signal intensity exhibited a number-dependent manner. These findings demonstrate that in situ synthetic barium sulfate nanocrystals endow the Cat27-CA/BS MCs with superior X-ray attenuation performance and huge potential applications in CT contrast imaging in vivo.

Mucoadhesive performance of Cat27-CA/BS MCs in vitro

To investigate the mucoadhesive properties of Cat27-CA/BS MCs, the binding behavior between catechol-grafted chitosan and mucin was first measured by SPR. SPR is a biosurface optical detection technique that studies the interaction between molecules and enables the precise quantitation and kinetic analysis of biomolecules.[41] When the refractive index of the substrate surface fluctuates, the format also changes accordingly. Therefore, SPR can be used to evaluate the adhesive capacity between catechol-grafted chitosan and mucin.[42] Calculations of immobilized mucin amounts are performed on the basis of the Biacore® standard relation: 1 response unit (RU) change corresponds to the sample volume changing by around 1 pg/mm^2. Figure 5 shows that the mucin solution was injected into the surface of the gold sensor for 10 minutes, which allowed mucin to adhere to the gold surface. Then, the gold surface was washed with PBS (pH 7.4), weakly adsorbed mucin was washed away, and covalently bound mucin remained. CS or Cat27-CS solution was injected until the signal was stable, when the mucin signal equilibrium was reached. In this test, response unit time increased to 1,608.1 seconds after injection of mucin, then after rinsing with PBS (pH 7.4), the response unit time of the gold surface decreased to 986.6 seconds. When CS solution was injected, the response unit time increased to 1,548.1 seconds. Under the same conditions, Cat27-CS solution increased the response unit time significantly to 2,848.9 seconds. Compared with CS, in which the ΔRU was 1,300.8 seconds, the protein quantity on the gold sensor surface increased by 1.30 ng/mm^2. The above finding fully demonstrates that Cat27-CS has more significant adhesive capacity on mucin than pure CS.[43]

Mucosa adhesion of Cat-CA/BS MCs in vitro

In view of the superior performance of catechol-grafted chitosan, the mucosa adhesion of as-prepared Cat27-CA/BS MCs was investigated using a wash-off test in vitro. First, a series of MCs was placed on the special surface coated with mucin. Then, the surface was slightly rinsed with PBS solution, and stranded MCs were counted for further analysis. As shown in Figure S3, the average relative retention rates of A/BS MCs as negative control and CA/BS MCs as the positive were 100% and 134%, respectively, indicating that chitosan with a positive charge could promote specific adhesion on a mucin-coated surface. Furthermore, the average relative retention rate of the Cat27-CA/BS MCs (166%) was higher than that of A/BS MCs and CA/BS MCs, verifying that catechol functionalization together with the positive charge polymer could further enhance the mucoadhesion. Based on these results, the prepared Cat27-CA/BS MSs exhibited superior adhesive performance on the mucosa coated surface.

Real-time CT imaging of Cat-CA/BS MCs in stomach

To investigate the imaging performance in vivo, mice were gavaged with Cat-CA/BS MCs and observed by CT scanning at different times ranged from 5 minutes to 48 hours.[44] Figure 6

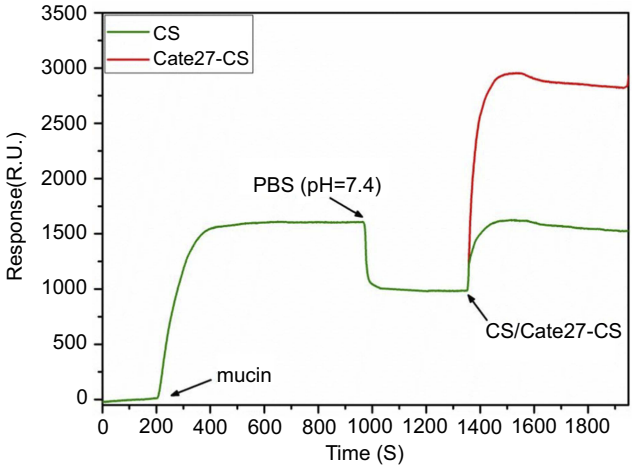

Figure 5 Evaluation of CS and Cate27-CS adhesive capacity on the mucin surface using SPR spectrum. The mucin solution was injected at the first arrow followed by a PBS wash and then CS (green solid line) and Cate27-CS solution (red solid line) were injected.
Abbreviations: CS, chitosan; Cat27, catechol-27.

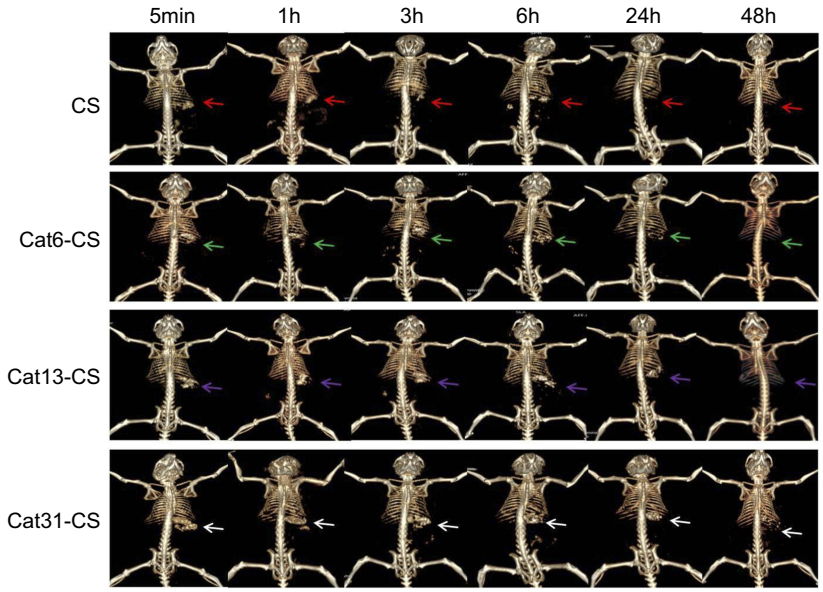

Figure 6 In vivo CT scanning images of mice at different times after oral administration of CA/BS MCs, Cat6-CA/BS MCs, Cat13-CA/BS MCs, Cat27-CA/BS MCs.
Abbreviations: CA/BS MCs, chitosan alginate/barium sulfate microcapsules; Cat-CA/BS MCs, catechol–chitosan alginate/barium sulfate microcapsules.

shows that after gavage for 5 minutes, 1 hour, and 3 hours, MCs could be observed in mouse stomach under all time periods, and very few could be found in the intestine. After 6 hours, the MCs started to migrate from the stomach to the gastrointestinal junction. After 24 hours, no MCs could be found in the stomach in the CA/BS MCs treatment group, and only a small amount in the Cat6-CA/BS MCs treatment group and about half in the Cat13-CA/BS MCs treatment group. Notably, a larger proportion of the MCs could be found in the stomach in the Cat27-CA/BS MCs treatment group. Furthermore, only Cat27-CA/BS MCs showed a clear retention of MCs in the mouse stomach at 48 hours, whereas MCs in the other groups had completely disappeared from the stomach and intestine. The above data demonstrate that the degree of catechol modification is positively correlated with the adhesion of the MCs to the mucosa. Meanwhile, the multifunctional MCs are verified to possess excellent CT imaging capabilities and can be used for real-time imaging tracking in vivo.

Verification of gastric retention of Cat-CA/BS MCs using NIR imaging

NIR fluorescence in vivo imaging technology has become an important method for in situ tracing, and has achieved good results in most studies.[45] To further verify the mucoadhesive properties of Cat-CA/BS MCs, the NIR fluorescence in vivo imaging technique was used to scan mice for fluorescence-labeled MCs for real-time imaging. Figure 7 shows that the fluorescence signal could be detected in each mouse at 6 hours, and remained in the stomach only in the Cat27-CA /BS MCs treatment group at 48 hours; otherwise, no signal was detected in the CA/BS MCs treatment group after 24 hours. It is thus confirmed that the catechol-modified MCs have better mucoadhesiveness.[46]

Cat-CA/BS MC-mediated RH sustained release for gastric ulcer treatment

Owing to the special physiological structure of the intestine, in situ gastrointestinal administration remains a huge challenge. Most stomach contents are discharged into the duodenum after 4–6 hours. The key to improving the therapeutic effect is to prolong the retention time of medication in the stomach. In this study, we chose gastric ulcer as a disease model to explore the sustained release feasibility of Cat27-CA/BS MC drugs in the stomach.[47] Photographs recorded images of the stomach after oral administration of DDW (control group), A/BS MCs, RH solution, RH-CA/BS MCs, and RH-Cat27-CA/BS MCs for 7 days in ulcer-induced KM mice (Figure S4). The antral wall structure and mucosa were obviously damaged, and congestion and edema were observed in the gastric mucosa of untreated mice. In addition, partial bleeding points and tissue edema were observed in the stomach of mice treated with pure MCs, and local gastric mucosa was slightly

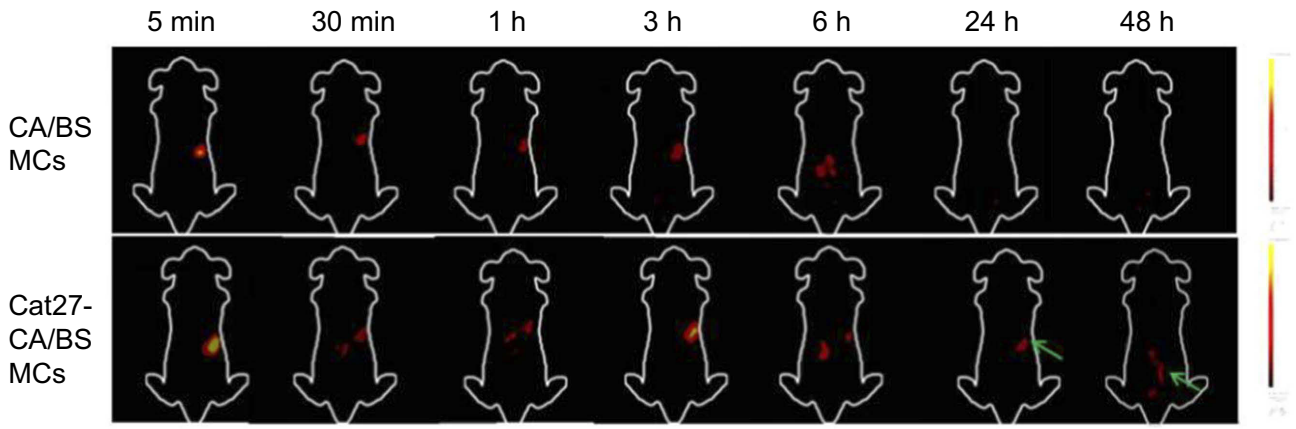

Figure 7 Near-infrared images of CA/BS MCs and Cat27-CA/BS MCs in real-time imaging tracer in vivo.
Abbreviations: CA/BS MCs, chitosan alginate/barium sulfate microcapsules; Cat27-CA/BS MCs, catechol-27–chitosan alginate/barium sulfate microcapsules.

atrophied. However, the mice in the other drug-administered groups had no obvious ulcerative damage of the gastric mucosa to the naked eye.

Many factors affect drug release in the carrier. To study the performance of drug release from MCs, we conducted release studies on drug-loaded MCs and MSs in vitro.[48] The simulated gastric fluid was chosen as the release medium and the cumulative release time was 18 hours. Figure 8A shows that the cumulative release rates of RH in the Cat27-CA/BS MSs group and Cat27-CA/BS MCs group in 1 hour were 22.69±5.75% and 32.63±0.81%, respectively; the release rate was fast at this stage. Then, the cumulative release of the RH in the Cat27-CA/BS MCs group reached about 50% in 3 hours, but that in the Cat27-CA/BS MSs group reached about 50% in 6 hours. Thereafter, the release rate of RH in both groups slowed down. At 18 hours, the cumulative drug release rate of RH in the Cat27-CA/BS MSs group was 72.33±0.22%, and that in the Cat27-CA/BS MCs was 90.74±4.59%. The in vitro release was consistent with first-order kinetics throughout the release process. It could be seen that the release rate of the drug in the MCs group was slightly faster than that in the MSs group, and the drug-loaded MCs could release more drugs in a certain period of time, more effectively maintaining the drug concentration compared with the MSs group. The MCs can fully release drugs and reduce residual drug in the capsules. Figure 8B shows the changes in body weight of mice in each group. Mice in the normal group had a healthy growth. Weight and activity in the gastric ulcer model group and the A/BS MCs treated group continued to decrease, and the back hair lacked luster. Body weight in mice treated with RH solution, RH-CA/BS MCs, and RH-Cat27-CA/BS MCs also decreased in the first 3–4 days, but gradually recovered in 4–5 days, and started to increase in the next 3 days. The mental state of the mice improved, their activity increased, and they drank water as normal. It could be effectively demonstrated that the prepared gastric adhesion type RH-Cat27-CA/BS MCs had certain therapeutic effects on gastric ulcer in mice. Figure 8C shows a bar graph of the weight of the whole stomach after 7 days' treatment in each group of mice. There were no significant differences among the groups. Figure 8D shows that the corresponding ulcer indices (control is recorded as 0) of different treatment groups were 15.5±6.6, 14.0±3.7, 11.8±3.8, 8.3±2.8, and 6.0±0.8. Compared with the single RH group, the ulcer inhibition rate of the RH-CA/BS MCs treatment group reached 46.26%, and that of the RH-Cat27-CA/BS MCs treatment group reached 61.29%. This effective gastric ulcer repair was most likely the result of a sustained slow release of the drug in the stomach.[49]

Figure 9 shows a section of gastric mucosa tissue of each treatment group. In the normal group, the stomach tissue was intact, the mucosa glands were arranged neatly, and no obvious inflammatory cell infiltration was observed. In the gastric ulcer model group and the A/BS MCs treatment group, ulcers were obvious, the cells in each layer were disordered, the mucosa layer was thin, some areas showed mucosal defects, a large number of inflammatory cells had infiltrated the submucosa, inflammatory exudation and necrosis was found on the surface, and some defects had spread to the bottom layer. Mucosal damage repair was not obvious. In the RH group, RH-CA/BS MCs group, and RH-Cat27-CA/BS MCs group, the ulcer was gradually relieved, the cells in each layer were regenerated, the mucosa layer

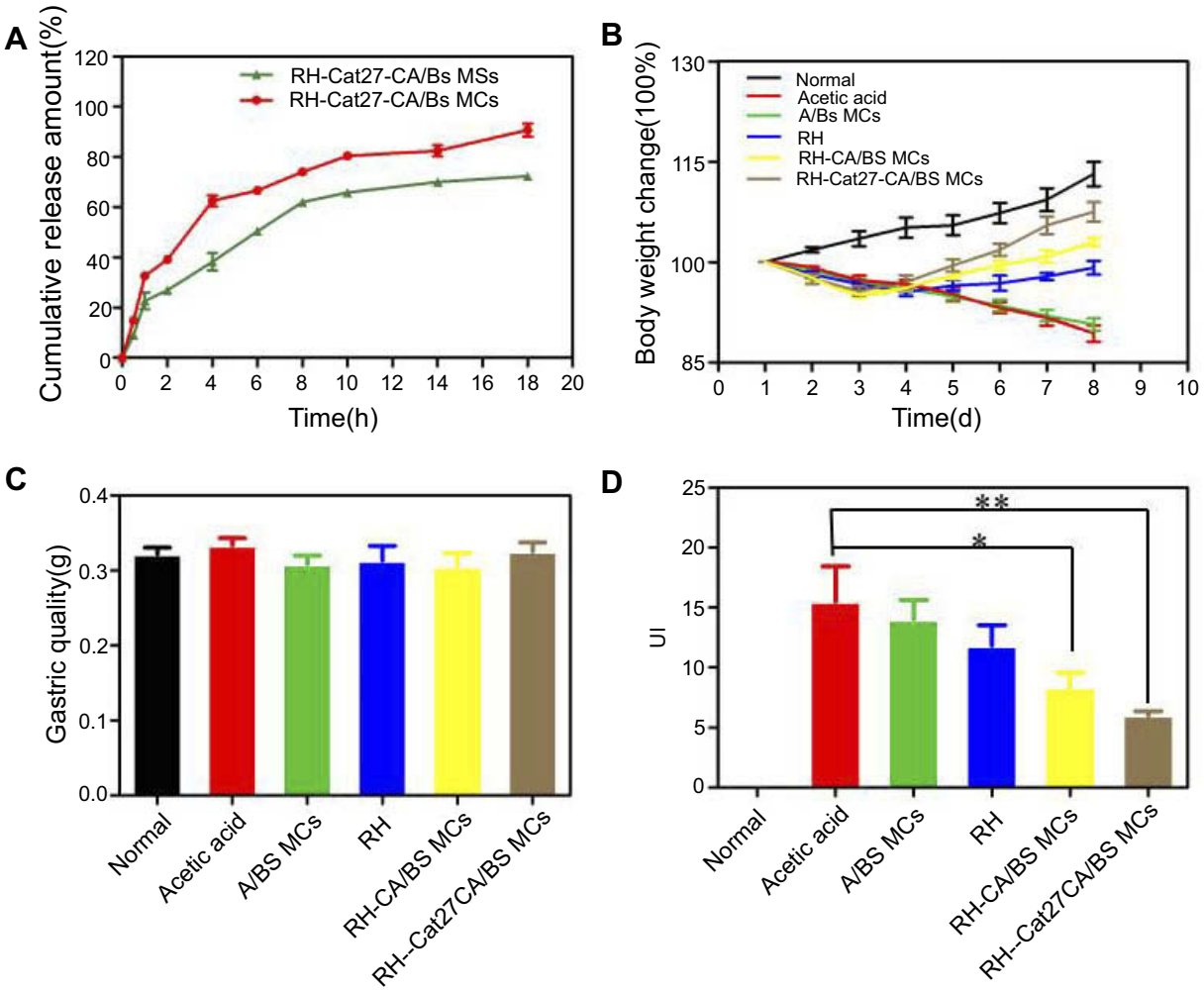

Figure 8 Catechol-functionalized alginate/barium sulfate multifunctional microcapsules mediated RH delivery for acetic acid-induced mouse gastric ulcer treatment. (**A**) Release curve of RH-Cat27-CA/BS MSs/MCs in simulated gastric fluid. (**B**) Loss of basal body weight of mice under different treatments during gastric ulcer disease. (**C**) Gastric weight from each group of mice under different treatments (n=6 per group). (**D**) UI for each group of mice under different treatments (n=6 per group). Data are presented as mean ± standard error of the mean. **P*<0.05, ***P*<0.01 vs acetic acid-alone-treated group on the same day.

Abbreviations: RH, ranitidine hydrochloride; Cat27-CA/BS MSs/MCs, catechol-27–chitosan alginate/barium sulfate microspheres/microcapsules; A/BS MCs, alginate/barium sulfate microcapsules; UI, ulcer index.

was thickened, and the inflammatory cells gradually became fewer, showing the effect of mucosal damage repair.

Discussion

Catechol-conjugated chitosan is one of a new generation of mucoadhesive polymers with long-lasting mucoadhesive and water-soluble properties for mucoadhesive drug delivery. In this study, the catechol moiety was conjugated to the side chain of chitosan by NHS chemistry. The modification method is affected by many factors, and the pH of the reaction environment plays an important role in the final degree of grafting. The grafting yield of catechol determines the adhesiveness of the catechol–chitosan composite to the mucosa. The more catechol it contains, the better the adhesion performance. Preparation of high-modification catechol–chitosan composites is an important prerequisite for the construction of mucoadhesive multifunctional MCs. In addition, barium ions play two roles in the formation of MSs and sulfate nanoclusters. On the one hand, the barium ions can undergo ion-exchange reactions with the sodium alginate in the molecular G unit, so that it accumulates and forms the hydrogel structure, thereby transforming into an MS after electrostatic spraying. On the other hand, barium sulfate crystals are formed by the combination of barium ions and sulfate ions, can be used as an X-ray contrast agent for digestive organs, and may be a good imaging tracer.

Traditional pharmaceutical preparations have some shortcomings, in that they are only released at a certain position after oral administration into the digestive tract, and a high concentration of the drug is formed in a short

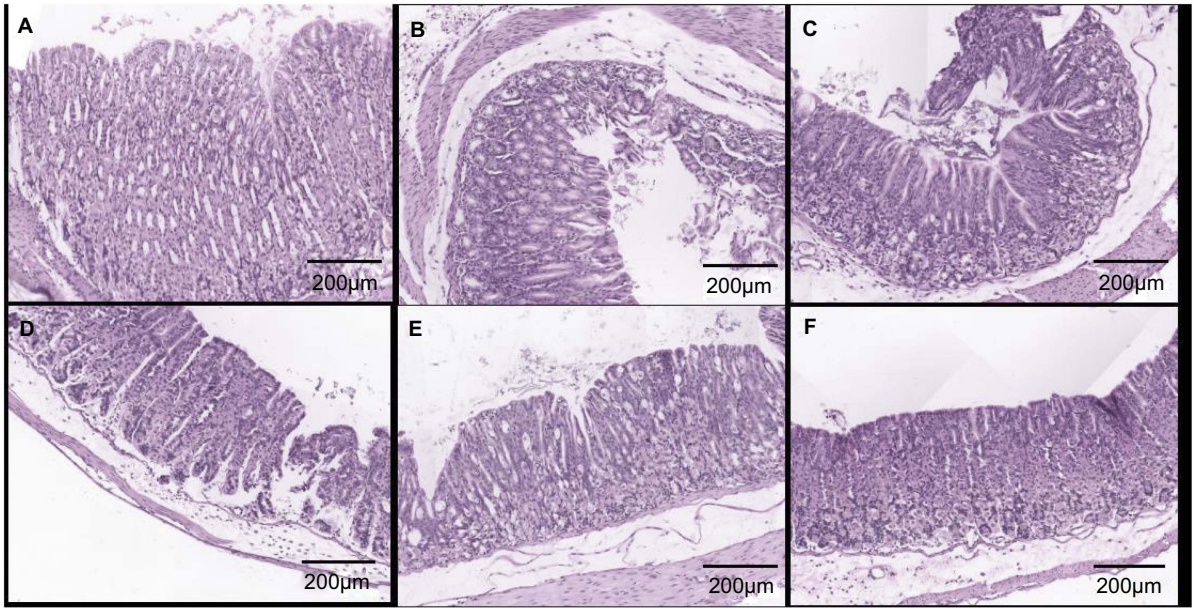

Figure 9 Pathological analysis of gastric tissues after distinct treatments using H&E staining assay after acetic acid induction. Magnification 100×. (**A**) Normal control. (**B**) Acetic acid induction. (**C**) A/BS MCs treatment. (**D**) RH treatment. (**E**) CA/BS MCs loading RH treatment. (**F**) Cat27-CA/BS MCs loading RH treatment.
Abbreviations: A/BS MCs, alginate/barium sulfate microcapsules; RH, ranitidine hydrochloride; CA/BS MCs, chitosan alginate/barium sulfate microcapsules.

period of time. This sudden release is not conducive to the sufficient absorption of the drug by the digestive tract. To address these shortcomings, in this study MCs were designed and prepared via a bionics strategy. The mucoadhesive MCs can prolong the retention effect by adhering to the mucosal surface, sustain the release of the drug at the corresponding site, control the drug release rate, reduce the fluctuation of the peaks and valleys of the drug's concentration in the blood, and enable the drug to continue to work smoothly. The novel gastric mucosal-retaining drug-loaded MCs have been prepared to overcome the defects of non-specific burst release of the drug. They can effectively adhere to the surface of the gastric mucosa and thereby stay in the stomach, and release the drug continuously and slowly, greatly improving the bioavailability of the drug and the therapeutic effect on gastric ulcers.

Conclusion

We have successfully developed a multifunctional Cat-CA/BS MC via catechol functionalization and in situ synthesis of barium sulfate nanoclusters for mucosal drug delivery and non-invasive real-time tracking in vivo. Inspired by the chemistry of mussel adhesion, catechol was successfully grafted onto the chitosan side chain with low, medium, and high degrees of modification to enhance the mucoadhesive performance. Then, these Cat-CSs were assembled on the surface of alginate microspheres with barium sulfate. The as-synthesized Cat-CA/BS MCs exhibited uniform size distribution and a spherical core–shell structure. After catechol conjugation, Cat-CA/BS MCs exhibited superior adhesive properties on the mucosa coated surface in vitro. In situ synthesis of barium sulfate nanoclusters on the inside of Cat-CA/BS MCs possessed similar phase structure to standard barium sulfate crystals, X-ray attenuation coefficients resulted in good CT imaging ability in vivo and in vitro, real-time positioning of MCs was achieved, and the visual research of drugs was realized. After oral administration, Cat27-CA/BS MCs displayed outstanding visibility under X-ray scanning for up to 24 hours, which further proved their long retention time in the stomach. Furthermore, the Cat-CA/BS MCs with a multilayered outer shell layer had greater toughness and stability than single-layer MCs, which could further achieve the sustained release of drug molecules in the target area. By loading RH as a model drug, Cat-CA/BS MCs with mucoadhesive properties showed longer retention time in the gastric area and better therapeutic effects on gastric ulcers than ordinary MCs. In view of these advantages, the resulting Cat-CA /BS MCs have huge application potential as multifunctional carriers in long-term drug delivery in the stomach and as non-invasive real-time monitoring features.

Acknowledgments

This work was supported by the Jiangsu 333 High-Level Talents Training Project (number BRA2017145), Six Talent

Peaks Project in Jiangsu Province (WSN-281), Key Talents of Medical Science in Jiangsu Province Project (QNRC2016444), the China Postdoctoral Science Foundation (2015M571705), and Zhenjiang Key Research and Development Program–Social Development (SH2016027).

Disclosure

The authors report no conflicts of interest in this work.

References

1. Xiong X, Sanmin HE, Shi S. Progress in the study of the novel gastroretentive drug delivery system. *Chin J Mod Appl Pharm*. 2011;28(11):988–994.
2. Mandal UK, Chatterjee B, Senjoti FG. Gastro-retentive drug delivery systems and their in vivo success: a recent update. *Asian J Pharm Sci*. 2016;11(5):575–584. doi:10.1016/j.ajps.2016.04.007
3. Coffin MD, Burke MD. Controlling Release by Gastroretention [M]// *Controlled Release in Oral Drug Delivery*. Springer US, 2011.
4. Klausner EA, Lavy E, Friedman M, Hoffman A. Expandable gastroretentive dosage forms. *J Control Release*. 2003;90(2):143–162. doi:10.1016/S0168-3659(03)00203-7
5. Kotreka UK, Adeyeye MC. Gastroretentive floating drug-delivery systems: a critical review. *Crit Rev Ther Drug*. 2011;28(1):47–99. doi:10.1615/CritRevTherDrugCarrierSyst.v28.i1.20
6. Rakesh P, Nidhi S, Vipin K, Kanchan K. Chitosan-based gastroretentive floating drug delivery technology: an updated review. *Expert Opin Drug Deliv*. 2012;9(5):525–539. doi:10.1517/17425247.2012.673581
7. Beom JK, Taegyun P, Hee CM, et al. Cytoprotective alginate/polydopamine core/shell microcapsules in microbial encapsulation. *Angewandte Chemie*. 2015;126(52):14671–14674.
8. Ghaffarian R, Herrero EP, Oh H, et al. Chitosan-alginate microcapsules provide gastric protection and intestinal release of ICAM-1-targeting nanocarriers, enabling GI targeting in vivo. *Adv Funct Mater*. 2016;26(20):3373. doi:10.1002/adfm.201670123
9. Mei L, He F, Zhou RQ, et al. Novel intestinal-targeted ca-alginate-based carrier for pH-responsive protection and release of lactic acid bacteria. *Acs Appl Mater Inter*. 2014;6(8):5962–5970. doi:10.1021/am501011j
10. Freiberg S, Zhu XX. Polymer microspheres for controlled drug release. *Int. J. Pharm*. 2004;282(1):1–18. doi:10.1016/j.ijpharm.2004.04.013
11. Fang Z, Jiang R, Zhang L, et al. In situ fabrication of radiopaque microcapsules for oral delivery and real-time gastrointestinal tracking of bifidobacterium. *Int J Nanomed*. 2018;13:4093–4105. doi:10.2147/IJN.S145837
12. Lee H, Dellatore SM, Miller WM, Messersmith PB. Mussel-inspired surface chemistry for multifunctional coatings. *Science*. 2007;318(5849):426–430.
13. Kim K, Kim K, Ryu JH, Lee H. Chitosan-catechol: a polymer with long-lasting mucoadhesive properties. *Biomaterials*. 2015;52(1):161–170. doi:10.1016/j.biomaterials.2015.02.010
14. Kim K, Ji HR, Dong YL, Lee H. Bio-inspired catechol conjugation converts water-insoluble chitosan into a highly water-soluble, adhesive chitosan derivative for hydrogels and LbL assembly. *Biomater Sci-Uk*. 2013;1(7):783–790. doi:10.1039/c3bm00004d
15. Lee Y, Chung HJ, Yeo S, et al. Thermosensitive, injectable, and tissue adhesive sol–gel transition hyaluronic acid/pluronic composite hydrogels prepared from bio-inspired catechol-thiol reaction. *Soft Matter*. 2010;6(5):977–983. doi:10.1039/b919944f
16. Maier GP, Rapp MV, Waite JH, Israelachvili JN, Butler A. Adaptive synergy between catechol and lysine promotes wet adhesion by surface salt displacement. *Science*. 2015;349(6248):628–632. doi:10.1126/science.aab0556
17. Yamagishi K, Kirino I, Takahashi I, et al. Tissue-adhesive wirelessly powered optoelectronic device for metronomic photodynamic cancer therapy. *Nature Biomed Eng*. 2018;3:27–36. doi:10.1038/s41551-018-0261-7
18. Lu H, Liu K, Wang M, et al. Mussel-inspired adhesive and conductive hydrogel with long-lasting moisture and extreme temperature tolerance. *Adv Funct Mater*. 2018;28(3):1704195. doi:10.1002/adfm.201704195
19. Liao M, Wan P, Wen J, et al. Wearable, healable, and adhesive epidermal sensors assembled from mussel-inspired conductive hybrid hydrogel framework. *Adv Funct Mater*. 2017;27(48):1703852. doi:10.1002/adfm.201703852
20. Xu J, Strandman S, Zhu JX, Barralet J, Cerruti M. Genipin-crosslinked catechol-chitosan mucoadhesive hydrogels for buccal drug delivery. *Biomaterials*. 2015;37:395–404. doi:10.1016/j.biomaterials.2014.10.024
21. Kalifa LG, Koehler RE, Margulis AR, Goldberg HI, Stoughton JA, Gibson RD. Use of substrate-coated barium sulfate tablets in the evaluation of digestive enzyme deficiency. *Radiology*. 1976;120(2):303–306. doi:10.1148/120.2.303
22. Ryu JH, Hong S, Lee H. Bio-inspired adhesive catechol-conjugated chitosan for biomedical applications: a mini review. *Acta Biomater*. 2015;27:101–115. doi:10.1016/j.actbio.2015.08.043
23. Lević S, LijakovićI P, Đorđević V, et al. Characterization of sodium alginate/D-limonene emulsions and respective calcium alginate/D-limonene beads produced by electrostatic extrusion. *Food Hydrocolloid*. 2015;45:111–123. doi:10.1016/j.foodhyd.2014.10.001
24. Hemant KSY, Singh MN, Shivakumar HG. Chitosan/sodium tripolyphosphate cross linked microspheres for the treatment of gastric ulcer. *Der Pharmacia Lettre*. 2010;2(3):106–116.
25. Lin YH, Tsai SC, Lai CH, et al. Genipin-cross-linked fucose-chitosan/heparin nanoparticles for the eradication of helicobacter pylori. *Biomaterials*. 2013;34(18):4466–4479. doi:10.1016/j.biomaterials.2013.02.028
26. Mohamed E, Hashim IA, Yusif R, et al. Polymeric micelles for potentiated antiulcer and anticancer activities of naringin. *Int J Nanomed*. 2018;13:1009–1027. doi:10.2147/IJN.S154325
27. Shi XY, Wang WJ, Li CL. Content determination of ranitidine hydrochloride in compound ranitidine capsules by HPLC. *Cent South Pharm*. 2013;11(8):613–616.
28. Tang S, Hao J. Determine the related substances of the preparations of ranitidine hydrochloride by HPLC. *Tianjin Pharm*. 2007;19(6):12–14.
29. Kobayashi T, Ohta Y, Yoshino J, Nakazawa S. Teprenone promotes the healing of acetic acid-induced chronic gastric ulcers in rats by inhibiting neutrophil infiltration and lipid peroxidation in ulcerated gastric tissues. *Pharmacol Res*. 2001;43(1):23–30. doi:10.1006/phrs.2000.0748
30. Kang GD, Lee SY, Jang SE, et al. Irisolidone attenuates ethanol-induced gastric injury in mice by inhibiting the infiltration of neutrophils. *Mol Nutr Food Res*. 2016;61(2):517–523.
31. Breviglieri E, Mota DSL, Boeing T, et al. Gastroprotective and anti-secretory mechanisms of 2-phenylquinoline, an alkaloid isolated from galipea longiflora. *Phytomedicine*. 2016;25:61–70. doi:10.1016/j.phymed.2016.12.016
32. Berenguer B, Alarcón DLLC, Moreno FJ, Martín MJ. Chronic gastric ulcer healing in rats subjected to selective and non-selective cyclooxygenase-2 inhibitors. *Eur J Pharmacol*. 2002;442(1–2):125. doi:10.1016/S0014-2999(02)01494-2
33. Cheng S, Yan D, Chen JT, et al. Soft-template synthesis and Characterization of ZnO_2 and ZnO hollow spheres. *J Phys Chem C*. 2009;113(31):13630–13635. doi:10.1021/jp9036028

34. Mi FL, Sung HW, Shyu SS, et al. Synthesis and characterization of biodegradable TPP/genipin co-crosslinked chitosan gel beads. *Polymer*. 2003;44(21):6521–6530. doi:10.1016/S0032-3861(03)00620-7
35. Ofner J, Krüger HU, Grothe H, et al. Physico-chemical characterization of SOA derived from catechol and Guaiacol-A model substance for the aromatic fraction of atmospheric HULIS. *Atmos Chem Phys*. 2011;11(1):1–15. doi:10.5194/acp-11-1-2011
36. Zvarec O, Purushotham S, Masic A, Ramanujan RV, Miserez A. Catechol-functionalized chitosan/iron oxide nanoparticle composite inspired by mussel thread coating and squid beak interfacial chemistry. *Langmuir the Acs J Surf Colloids*. 2013;29 (34):10899–10906. doi:10.1021/la401858s
37. Lópezmartínez LM, Santacruzortega H, Navarro RE, et al. A ^{1}H NMR Investigation of the interaction between phenolic acids found in mango (*Manguifera Indica Cv Ataulfo*) and papaya (*Carica Papaya Cv Maradol*) and 1,1-diphenyl-2-picrylhydrazyl (DPPH) free radicals. *PLoS One*. 2015;10(11):e0140242. doi:10.1371/journal.pone.0140242
38. Vigo D, Villani S, Faustini M, et al. Follicle-like model by granulosa cell encapsulation in a barium alginate-protamine membrane. *Tissue Eng*. 2005;11(5–6):709–714. doi:10.1089/ten.2005.11.709
39. Link TW, Arifin DR, Long CM, et al. Use of magnetocapsules for in vivo visualization and enhanced survival of xenogeneic HepG2 cell transplants. *Cell Med*. 2012;4(2):77–84. doi:10.3727/215517912X653337
40. Wang X, Shi J, Jiang Z, et al. Preparation of ultrathin, robust protein microcapsules through template-mediated interfacial reaction between amine and catechol groups. *Biomacromolecules*. 2013;14 (11):3861–3869. doi:10.1021/bm400426f
41. Thongborisute J, Takeuchi H. Evaluation of mucoadhesiveness of polymers by BIACORE method and mucin-particle method. *Int J Pharmaceut*. 2008;354(1):204–209. doi:10.1016/j.ijpharm.2007.12.001
42. Thongborisute J, Takeuchi H, Yamamoto H, Kawashima Y. Properties of liposomes coated with hydrophobically modified chitosan in oral liposomal drug delivery. *Pharmazie*. 2006;61 (2):106–111.
43. Bravo-Osuna I, Noiray M, Briand E, et al. Interfacial interaction between transmembrane ocular mucins and adhesive polymers and dendrimers analyzed by surface plasmon resonance. *Pharm Res-Dordr*. 2012;29(8):2329–2340. doi:10.1007/s11095-012-0761-1
44. Arifin DR, Long CM, Gilad AA, et al. Trimodal gadolinium-gold microcapsules containing pancreatic islet cells restore normoglycemia in diabetic mice and can be tracked by using US, CT, and positive-contrast MR imaging. *Int J Med Radiol*. 2011;260 (3):790–798.
45. Gao N, Bozeman EN, Qian W, et al. Tumor Penetrating theranostic nanoparticles for enhancement of targeted and image-guided drug delivery into peritoneal tumors following intraperitoneal delivery. *Theranostics*. 2017;7(6):1689–1704. doi:10.7150/thno.18125
46. Wang R, Zhou L, Wang W, et al. In vivo gastrointestinal drug-release monitoring through second near-infrared window fluorescent bioimaging with orally delivered microcarriers. *Nature Commun*. 2017;8:14702. doi:10.1038/ncomms14702
47. Yang XL, Ju XJ, Mu XT, et al. Core-shell chitosan microcapsules for programmed sequential drug release. *Acs Appl Mater Inter*. 2016;8 (16):10524. doi:10.1021/acsami.6b01277
48. Duncan TV, Karthik P. Release of engineered nanomaterials from polymer nanocomposites: diffusion, dissolution, and desorption. *Acs Appl Mater Inter*. 2015;7(1):2–19. doi:10.1021/am5062745
49. Alai M, Wen JL. Application of nanoparticles for oral delivery of acid-labile lansoprazole in the treatment of gastric ulcer: in vitro and in vivo evaluations. *Int J Nanomed*. 2015;10:4029.

Supplementary materials

Experimental section

1. Materials and characterization

Materials

Fluorescein 5(6)-isothiocyanate and rhodamine B were purchased from Aladdin Industrial Inc.

Characterization

Laser scanning confocal microscopy (LSCM) was carried out on an FV1200 (Japan).

2. Synthesis of FITC-alginate and rhodamine B–chitosan

100 mL of 2.5% sodium alginate solution, pH adjusted to 8.5 with 1 N sodium hydroxide; 100 μL of FITC (1 mg/mL) solution dissolved in DMSO was added, then incubated at 40°C for 1 hour, followed by dialysis against light (molecular weight cut-off: 1,000) for 2 days.

1% chitosan solution was dissolved in 0.1 mol/L acetic acid; 50 μL of rhodamine B (0.5 mg/mL) solution dissolved in DMSO was added, then incubated for 30 minutes at room temperature with stirring, followed by dialysis against light (molecular weight cut-off: 1,000) for 2 days.

3. Characteristics of multiple coatings on the MC shell

FITC-alginate and rhodamine B–chitosan were scanned using a laser confocal microscope and the multilayer coating on the outer wall of the MCs was localized by fluorescence.

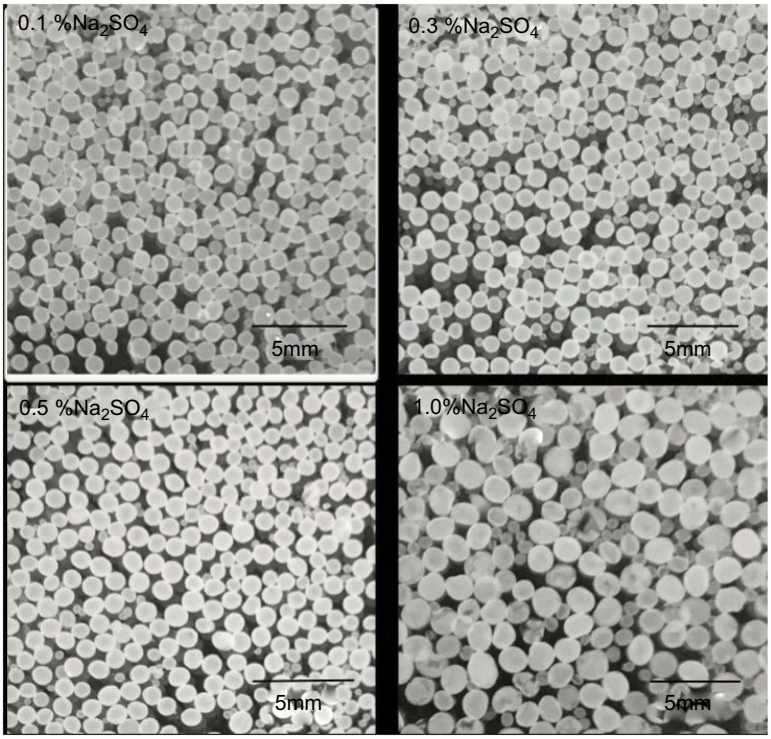

Figure S1 Effect of sodium sulfate at different concentrations from 0.1% to 1.0% on the morphology of catechol 27–chitosan alginate/barium sulfate microcapsules.

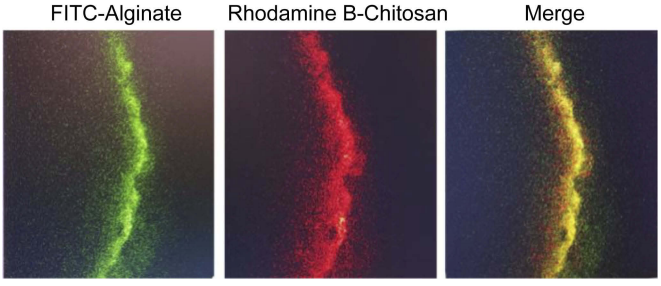

Figure S2 Laser scanning confocal microscopy images of a wall section of catechol-27–chitosan/barium sulfate microcapsules under different excitation wavelengths.
Abbreviation: FITC, fluorescein isothiocyanate.

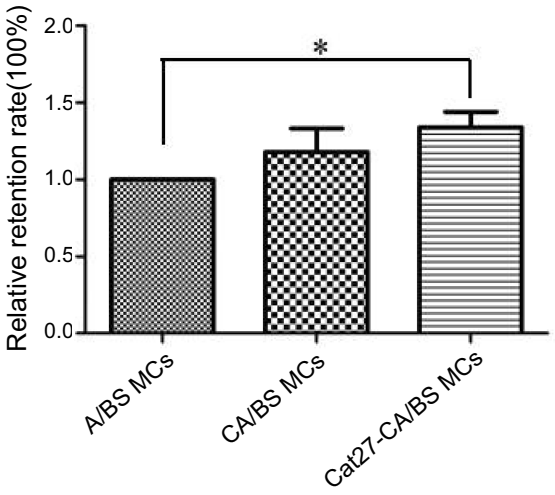

Figure S3 Relative retention rates of A/BS MCs, CA/BS MCs, and Cat27-CA/BS MCs (n=5 per group) on the mucin-coated surface after PBS washing.
Note: *Significant differences.
Abbreviations: A/BS MCs, alginate/barium sulfate microcapsules; CA/BS MCs, chitosan alginate/barium sulfate microcapsules; Cat27-CA/BS MCs, catechol-27–chitosan alginate/barium sulfate microcapsules.

Acetic acid	-	+	+	+	+	+
RH	-	-	+	-	+	+
MC_s	-	-	-	+	+	-
Cat27-CA/BS MC_s	-	-	-	-	-	+

Figure S4 Macroscopic appearance and area of acetic acid-induced gastric ulcer after different treatments: normal; acetic acid; alginate/barium sulfate microcapsules (A/BS MCs); ranitidine hydrochloride (RH); ranitidine hydrochloride–chitosan alginate/barium sulfate microcapsules (RH-CA/BS MCs); and ranitidine hydrochloride–catechol-27–chitosan alginate/barium sulfate microcapsules (RH-Cat27-CA/BS MCs).